Structural stability of Co-V intermetallic phases and thermodynamic description of the Co-V system

Peisheng Wang[1], Thomas Hammerschmidt[2], Ursula R. Kattner[3], Gregory B. Olson[1]

1, Center for Hierarchical Materials Design (CHiMaD), Northwestern University, 2205 Tech Drive, Evanston, IL 60208

2, Interdisciplinary Centre for Advanced Materials Simulation (ICAMS), Ruhr-Universität Bochum, 44801 Bochum, Germany

3, Materials Science and Engineering Division, National Institute of Standards and Technology, 100 Bureau Dr., MS 8555, Gaithersburg, MD 20899

Abstract

The Co-V system has been reviewed. Density functional theory (DFT) calculations using the generalized gradient approximation (GGA) were used to obtain the energies for the end-members for all three intermediate phases, Co_3V, σ and CoV_3. Results from DFT calculations considering spin polarization were used to evaluate the CALPHAD (Calculation of phase diagrams) model parameters. The method to evaluate the contribution of the magnetism to the energies of Co-rich compounds that was introduced in our previous work is presented in more detail in the present work. For the description of the σ phase, the magnetic part of the total energy is included in the description of the pure Co end-member compound resulting in a non-linear description of the magnetic contribution over composition. The calculated phase diagram obtained from the present CALPHAD description is in good agreement with the experimental data. The metastable FCC-$L1_2$ phase diagram was calculated and compared with experimental data.

Keywords

Co-V, thermodynamics, phase diagram, magnetism; σ phase; $L1_2$, superalloy

Introduction

Coherent precipitates of $L1_2$ (γ') phase in the face centered cubic (FCC, A1, γ) matrix are the reason that Ni-based superalloys can maintain strength at high temperatures. Unlike the Ni-based superalloys where the strengthening phase, $L1_2$ Ni_3Al (γ'), is thermodynamically stable with a high melting point (above 1642 K) [1], the Co-Al $L1_2$ phase is not stable [2]. Searching for elemental combinations for a stable $L1_2$-γ' strengthening phase at typical service temperatures (≈1373 K) of a jet engine is one of the major objectives for the development of the new Co-based γ/γ' superalloys. Sato et al.[3] found that Co-Al-W alloys with ordered γ' ($L1_2$) phase precipitates in a γ phase matrix (FCC_A1) exhibited precipitation-hardened characteristics. However, it was then found that the ternary $L1_2$ Co_3(Al,W) phase is thermodynamically metastable [4-6]. Additional elements need to be added to stabilize the Co_3(Al,W) phase [7]. Although the addition of W can increase the temperature of the metastable γ/γ' solvus, additional W does not sufficiently stabilize the $L1_2$ phase [8]. Thus, searching for W-free ternary systems with a stable $L1_2$ phase seems to be a promising alternative route to Co-based γ/γ' superalloys. Nyshadham et al. [9] performed high-throughput density functional theory (DFT) calculations to screen for new ternary $L1_2$ compounds. They found that $L1_2$ is stable at 0 K in the Co-Nb-V and Co-Ta-V systems. However, subsequent experimental studies by Ruan et al. [10] and Reyes Tirado et al. [11] showed that the γ' phase is not stable above 1173 K in both Co-Nb-V and Co-Ta-V. An experimental study of the Co-Al-V system at 1073 K by Liao et al. [12] did not show the stable $L1_2$ in the Co-rich corner of the system. However, a more recent study by Chen et al. [13] of Co-Al-V based alloys found that the $L1_2$ phase is thermodynamically stable at 1173 K. The Co_3V phase with $L1_2$ structure, which is not a stable phase in the binary system [14], can be obtained by quenching. This indicates that the energy of $L1_2$ Co_3V should be close to the stable phase, hP24 Co_3V, which is confirmed by DFT calculation in the present work and in previous works [15, 16]. Thus, a thorough investigation of the phase equilibria of

the Co-V system including the metastable $L1_2$ phase is necessary for the further development of the Co-V based γ/γ' superalloys.

CALPHAD (Calculation of phase diagrams) type databases provide a set of self-consistent descriptions of the thermodynamic properties of multi-component systems [17] through critical assessment of the relevant binary and ternary systems. The Co-V system has been thermodynamically assessed by Bratberg and Sundman [18], Huang et al. [19] and Wang et al. [20]. The description from Bratberg and Sundman reproduces the evaluated experimental phase diagram from Smith [21] well. However, the model for the important topologically close-packed (TCP) σ phase was simplified and the model parameters were solely obtained from the available experimental information. Even more simplifications were used in the assessments of Huang et al. [19] and Wang et al. [20] which makes their descriptions unsuitable for the implementation in existing thermodynamic databases for Co-based γ/γ' superalloys. To obtain a reliable description for phases that may have significant homogeneity ranges in systems with three or more components, such as the σ phase, a reliable optimization of the model parameters using results from DFT calculations is essential.

The primary objective of the present work is to provide a thermodynamic description of the Co-V system employing results from DFT calculations that is well-suited for extending the thermodynamic database for Co-based γ/γ' superalloys under development [8]. In addition, the treatment proposed by Wang et al. [22] for the magnetic contribution to the total energy for the σ phase is discussed.

Literature Review

The experimental information published until 1989 was critically evaluated by Smith [21]. Smith accepted three intermediate compounds, (i) Co_3V with an ordered hexagonal superlattice structure, hP24, where the ordering within a close-packed layer is the same as in $L1_2$ but with a different layering sequence from that in $L1_2$, (ii) the σ

phase with CrFe ($D8_b$, tP30) structure and (iii) CoV_3 with Cr_3Si (A15, cP8) structure. Smith also reported the $L1_2$ structure for Co_3V to exist over a narrow temperature range (≈1295 K to 1343 K) between the hP24 hexagonal ordered Co_3V and disordered FCC-Co phases. Later, Nagel et al. studied the thermal stability of the Co_3V phase using in-situ neutron diffraction [14]. The in-situ neutron diffraction experiments were carried out between room temperature and 1333 K. The $L1_2$ phase that was found at low temperatures in the as-quenched alloy transformed upon heating to the hP24 phase and then directly to the FCC solid solution at high temperatures. The $L1_2$ phase was not observed to form again at any elevated temperature, even after annealing for several hours. It was then concluded that the $L1_2$ Co_3V is a not a stable phase in the Co-V system. The hP24 Co_3V transforms to FCC phase at about 1318 K (1312 K to 1323 K). The crystallographic information for the phases in the Co-V system is summarized in Table 1.

Wang et al. [20] has studied the phase equilibria of the Co-V system at 973 K using diffusion couples. However, the composition profile shown does not reveal clear differences in phase compositions at the phase boundaries which suggests that the determined compositions may have large errors and, therefore, the data were considered as semiquantitative in the present work.

No new experimental data for the thermodynamic properties of the phases in the Co-V system were published since the evaluation by Smith [21]. Hammerschmidt et al. [23] performed high-throughput first-principles calculations of the TCP phases in a number of binary systems, including Co-V. These calculations showed that the A15 and the σ phase are the only TCP phases that are expected in this binary system, in line with the experimental findings.

First-principles calculations

In the present work we report density-functional theory (DFT) calculations for all end-members of the $PuAl_3$, $L1_2$, CrSi (σ) and Cr_3Si (A15) phases as listed in Table 2. The results for the end-members of other TCP phases are given in the supplemental

material. For the calculations all Wyckoff sites with all possible stoichiometric configurations were considered. The corresponding total energy calculations were performed with the Vienna Ab initio Simulation Package (VASP)[1] [23-25] using projector augmented wave (PAW) pseudopotentials [26] with p semicore states for V and the generalized gradient approximation (GGA) [27]. The differences in the formation energies are converged to 1 meV/atom with a plane-wave cutoff of 400 eV and Monkhorst-Pack k-point meshes with 0.02 $Å^3$. Starting with an initially ferromagnetic spin arrangement, the structures are fully relaxed until the forces on the atoms are less than 0.01 eV/Å. These structures are subjected to volume changes of ±5 % to determine the cohesive energy and the equilibrium volume by fitting to the Birch-Murnaghan equation of state.

Thermodynamic CALPHAD modeling

Pure elements

The descriptions of the Gibbs energy of the pure elements as function of temperature $G_{\mathrm{Co}}^{\circ,\varphi}$ and $G_{\mathrm{V}}^{\circ,\varphi}$, are taken from the pure element thermodynamic database of the Scientific Group Thermodata Europe (SGTE) [28]. For Co and V the data in this database are identical to those compiled by Dinsdale [29].

Solution phases

The composition dependence of the Gibbs energy of the solution phases liquid, body centered cubic V (BCC_A2), face centered cubic αCo (FCC_A1), and hexagonal close packed εCo (HCP_A3) is described by a substitutional solution model with Redlich–Kister polynomials [30]. The magnetic contribution to the Gibbs energy of the solution phases is described with the Hillert-Jarl formalism [31]. In this formalism

[1] Commercial products are identified in this paper for reference. Such identification does not imply recommendation or endorsement by the National Institute of Standards and Technology, nor does it imply that the materials or equipment identified are necessarily the best available for the purpose.

the magnetic transformation temperature and magnetic moment are the input parameters to describe the contribution of the magnetism to the Gibbs energy. The composition dependence of these two parameters can also be described with Redlich-Kister polynomials.

Intermetallic compounds

The CoV_3 phase is modeled as simple stoichiometric compound:

$$G^{CoV_3} = 1°G_{Co}^{HSER} + 3°G_{Ta}^{HSER} + \Delta G_f^{CoV_3} \quad (1)$$

Where HSER normally stands for the reference state of the element, i.e., its stable form at 298.15 K and 1 bar. However, it must be pointed out that for the magnetic elements, such as Fe, Co or Ni, HSER stands for their paramagnetic state at 298.15 K and 1 bar. $\Delta G_f^{CoV_3} = A + B \cdot T$ represents the Gibbs energy of formation of the compound CoV_3 from the components Co and V, referred to $°G_{Co}^{HSER}$ and $3°G_V^{HSER}$.

For the first-principles calculations of the end-members of the σ phase, all occupation patterns of Co and V were considered for all five Wyckoff sites of the σ structure. For the development of the CALPHAD database the model was simplified to a three sublattice model, i.e. sites 2a and $8i_2$ are combined into one sublattice and sites $8i_1$ and 8j are combined into another one while site 4c is unmodified, resulting in $(Co,V)_{10}(Co,V)_4(Co,V)_{16}$. It should be noted that a five sublattice notation is used to identify results from the DFT calculations while a three sublattice notation is used for the CALPHAD parameters.

The extended Compound Energy Formalism (CEF) [32] was used to describe a configuration independent contribution to the Gibbs energy of the σ phase:

$$G_m^{\sigma} = G_m^{dis}(x_i) + \Delta G_m^{\text{conf}}\left(y_i^{(s)}\right) \quad (3)$$

$$G_m^{dis}(x_i) = \sum_i x_i \, {}^{\circ}G_i^{dis\_\sigma} + \sum_i \sum_{j>i} \sum_v x_i x_j \, (x_i - x_j)^v L_{i,j}^{v,\sigma} \quad (4)$$

$$\Delta G_m^{\text{conf}}\left(y_i^{(s)}\right) = \sum_i \sum_j \sum_k \Delta G_{i:j:k}^{\sigma} + RT \sum_s a^{(s)} \sum_i y_i^{(s)} \ln y_i^{(s)} \quad (5)$$

where x_i is the overall composition of the σ phase, $y_i^{(s)}$ is the fraction of site *s* occupied by element *i*, $a^{(s)}$ is the total number of sites corresponding to site *s* and ${}^{\circ}G_i^{dis\_\sigma}$ is the molar Gibbs energy of the hypothetical pure element *i* (Co, V) in *σ* structure, referred to Co-HCP and V-BCC without magnetic contribution. $\Delta G_{i:j:k}^{\sigma}$ is the molar Gibbs energy of formation of the stoichiometric end-member from the pure element with the Gibbs energy ${}^{\circ}G_i^{dis\_\sigma}$. G_{mag}^{σ} can be included in the description of the end-member compounds $\Delta G_{i:j:k}^{\sigma}$ or with the modified CEF as contribution to the Gibbs energy of the pure component, ${}^{\circ}G_i^{dis\_\sigma}$.

Describing the Co_3V phase as an ordered variant of the FCC structure would require a description with more than four sublattices in the order/disorder formalism of the Compound Energy Formalism (CEF) [33]. Since this ordered structure has been reported only in a few systems and does not play a significant role in the development of commercial alloys its homogeneity range was described using a simple CEF model with two sublattices, $(Co,V)_3(Co,V)_1$

The metastable ordering of the FCC phase is described using the four-sublattice order/disorder formalism [34].

Treatment of magnetism in CALPHAD modeling

For a phase with magnetism, the CALPHAD representation of the Gibbs energy uses a separate term (ΔG_{mag}) to describe the contribution from magnetism to the total energy. The ferromagnetic phase transforms into the paramagnetic state rather than to a state where the spins do not contribute to the total energy. Thus, the CALPHAD "non-magnetic" part of the Gibbs energy function actually describes the total Gibbs energy for the paramagnetic state. Results from DFT calculations are nowadays widely accepted as very useful input for CALPHAD assessments. However, DFT calculations for the paramagnetic state are still challenging due to the computational effort. Alternative approaches such as the disordered local moment (DLM) approach

based on the coherent potential approximation (CPA) [35, 36] are similarly demanding. Thus, in practice, the CALPHAD 'non-magnetic' part is often approximated by non-spin-polarized DFT calculations.

First principles calculations [36] show that the energy of paramagnetic HCP Co relative to ferromagnetic HCP Co is 19000 J/mol while that of non-magnetic HCP Co is 21500 J/mol (values digitized from graph). A survey of first-principles data for the Co-Cr system [22] has shown that the energy for the non-magnetic Co in the σ structure (from DFT) and the paramagnetic Co in σ structure by (DLM-CPA) are 34494 J/mol and 19460 J/mol, respectively. Both examples clearly illustrate that proper treatment of the magnetic contribution to the Gibbs energy is important. In our previous work [22] we introduced a method to describe the Gibbs energy of the end-members using DFT results for systems containing magnetic elements. The same method was applied in the present work. Since this method was only described briefly in [22] it will be described here in detail.

In general, only the results from DFT calculations considering spin-polarization are needed to set up an approximate CALPHAD description of the complex magnetic compounds containing Co.

For the description of the σ phase the first step is to evaluate the magnetic moment, β_{Co}^{σ}, and Curie temperature, $\mathrm{Tc}_{Co}^{\sigma}$, of pure Co with σ structure using the DFT results. The DFT value of the magnetic moment is used directly. The value from the present DFT calculation is 1.67 μ_B/atom which is consistent with the value from our previous work [22]. The Curie temperature for pure Co with σ structure is estimated on the basis of the Heisenberg model [37] with the assumption that the exchange integrals do not significantly change between HCP and σ phases of Co, i.e., $\frac{\mathrm{Tc}_{Co}^{\sigma}}{\mathrm{Tc}_{Co}^{HCP}} \approx \frac{\beta_{Co}^{\sigma}}{\beta_{Co}^{HCP}}$. resulting in an estimated Curie temperature of 1400 K. To be consistent with the previous assessment, the value β_{Co}^{σ}=1.66 μ_B/atom and $\mathrm{Tc}_{Co}^{\sigma}$=1400 K were adopted from [22].

The second step is to determine the magnetic contribution to the energy of the pure

Co in the σ form at 0 K. The Hillert-Jarl [31] formula was used to describe the magnetic contribution to the total energy. The magnetic moment β_{Co}^{σ} and Curie Temperature Tc_{Co}^{σ} are the only input parameters. The contribution of magnetism to the energy for Co in the σ phase at 0 K is

$$\Delta G_{Co,mag}^{\sigma} = -R\ln(\beta_{Co}^{\sigma}+1)\,(p_0 Tc_{Co}^{\sigma}) \quad (6)$$

with p_0 = 0.86034 for non-BCC phases gives $\Delta G_{Co,mag}^{\sigma}$=-9797.0 J/mol.

The third step is to evaluate ${}^{o}G_{Co}^{dis\_\sigma}$ for the paramagnetic state using:

$${}^{o}G_{Co}^{dis\_\sigma} = \Delta G_{Co:Co:Co:Co:Co}^{\sigma} - \Delta G_{Co,mag}^{\sigma} + \Delta G_{Co,mag}^{HCP} + {}^{\circ}G_{Co}^{HSER} \quad (7)$$

where $G_{Co,mag}^{HCP}$ represents the magnetic contribution to the Gibbs energy of HCP Co, which is taken from SGTE database and is -8532 J/mol at 0 K. $\Delta G_{Co:Co:Co:Co:Co}^{\sigma}$ is the DFT calculated enthalpy of formation for Co in the σ phase at 0 K. Although this value is less than half of the difference obtained from the first principles calculations [36] it was used here to ensure consistency of the description within the CALPHAD framework. ${}^{o}G_{Co}^{dis_\sigma}$was then determined as 6958 J/mol +${}^{\circ}G_{Co}^{HSER}$.

The next step is to describe the the contribution of the magnetism to the total energy over the composition range. As mentioned above, G_{mag}^{σ}can be included in the description of the end-member compound $\Delta G_{Co:Co:Co}^{\sigma}$ or with the modified CEF as a contribution to the Gibbs energy of the pure component, ${}^{\circ}G_{Co}^{dis\_\sigma}$. If G_{mag}^{σ} is part of ${}^{\circ}G_{Co}^{dis\_\sigma}$ without introducing any interaction parameter, the magnetic contribution to the total energy over composition will be linear. Figure 1 shows that the magnetic moment quickly decreases with decreasing Co-content and has almost disappeared for the region of the phase diagram where the σ phase is stable. This is also the case for other Co systems [22]. Thus, additional interaction parameters are necessary to fit the DFT results. Alternatively, G_{mag}^{σ} can be included in the description of the end-member compound $\Delta G_{Co:Co:Co}^{\sigma}$, which automatically results in a non-linear description of the

magnetic contribution Thus, in the present work, G^{σ}_{mag} is included in the description of the end-member compound $\Delta G^{\sigma}_{Co:Co:Co}$.

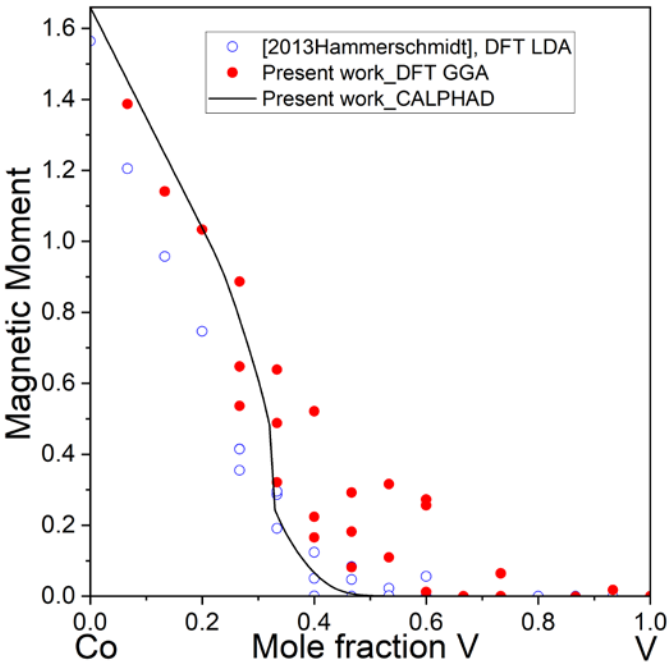

Fig.1 CALPHAD magnetic moment for the σ phase at 298.15 K compared with DFT calculated average moments at 0 K.

Results and discussion

The optimization of the model parameters of the Co-V system was performed using the PARROT module of the Thermo-Calc software [38]. Table 3 lists the phases, names, models, and parameters used in the present work.

To fit the $\Delta G^{\sigma}_{i:j:k} = A + BT$ parameters of the simplified 3 sublattice model of the σ phase, all of the 32 energy values from the DFT calculations were used. B parameters were only introduced when they were necessary to obtain better agreement with the experimental phase diagram.

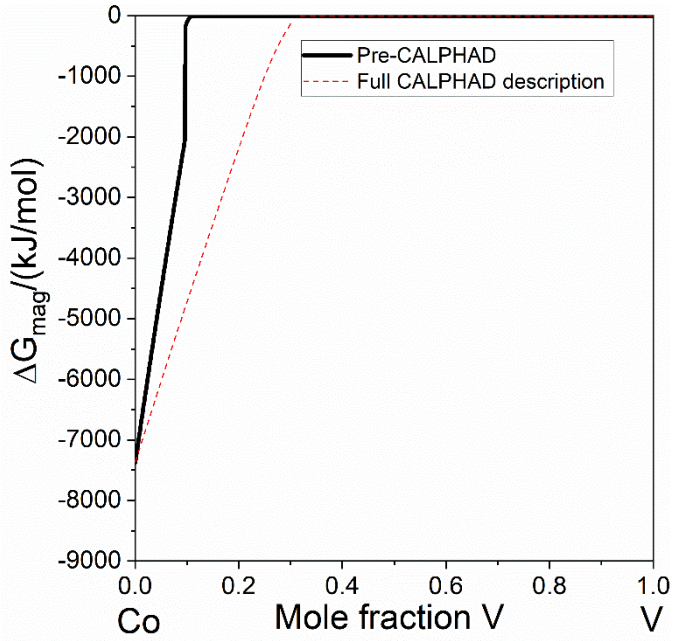

Fig.2 CALPHAD Curie temperature for the σ phase at 298.15 K compared with experimental data [39].

Figures 1 and 2 show the calculated magnetic moment and Curie temperature for the σ phase compared with the DFT values and experimental data [39], respectively. With only two magnetic parameters, β_{Co}^{σ}=1.66 μ_B/atom and Tc_{Co}^{σ}=1400 K, for the pure Co σ phase end-member the composition dependence of the magnetic moment and Curie temperature is well described. The calculated magnetic contribution to the total energy (ΔG_{mag}) for the σ phase is shown in Fig. 3. The solid black line represents the pre-assessment calculated ΔG_{mag} (no B values for the $\Delta G_{i:j:k}^{\sigma} = A + BT$ or

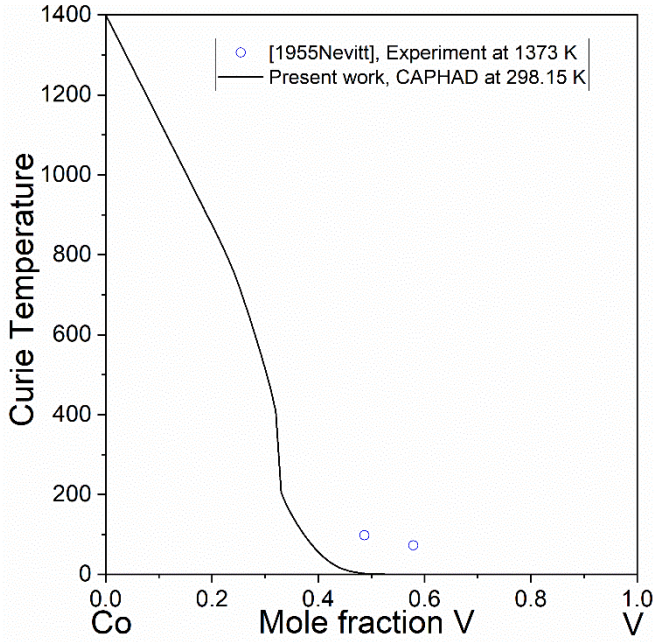

Fig.3 Calculated magnetic contribution to the total energy for the σ phase.

interaction parameters) while the red dashed line represents the calculated ΔG_{mag} after the CALPHAD assessment. Differences in the range of 0 V to 0.22 V result from the configurational ordering, as shown in Table 4. Table 4 lists the calculated site occupation of Co in the 3 sublattices and magnetic contribution for x(V) = 0.134 and T = 298.15 K to the total energy using pre-assessment and fully assessed parameters. It shows that the change of ΔG_{mag} is a result of the ordering of the σ phase. In the stable σ phase region, the magnetic contribution to the total energy is 0.

The calculated Co-V phase diagram is shown in Fig. 4, it can be seen that it agrees well with the experimental data. As discussed, the experimental data from Wang et al. [20] were only considered qualitatively. Thus, the present calculation shows large deviations from these data.

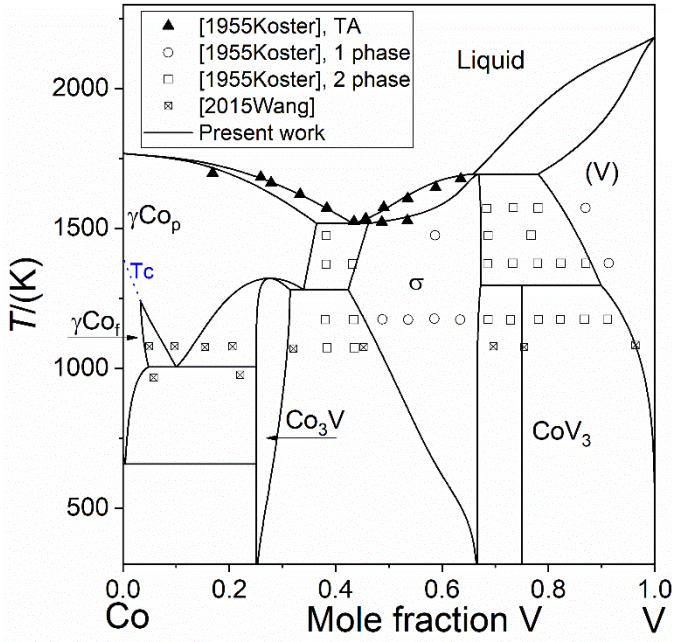

Fig.4 Calculated Co-V phase diagram compared with experimental data

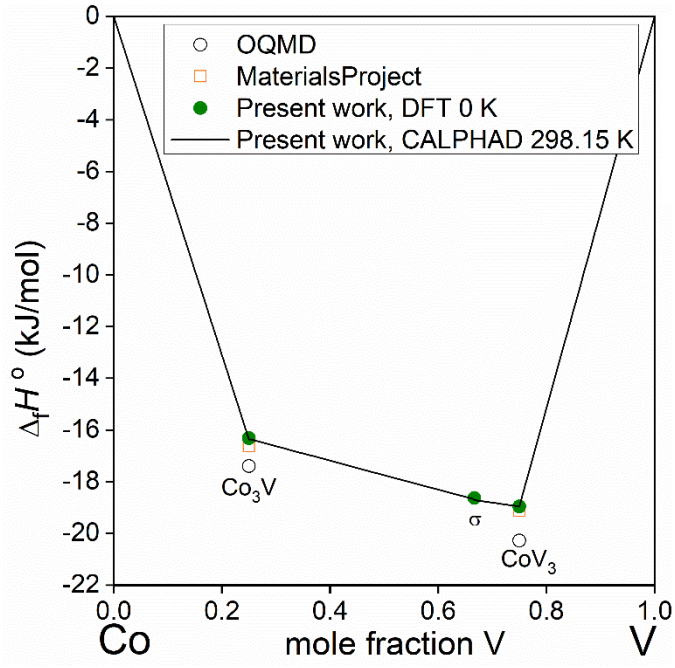

Fig.5 Calculated enthalpies of formation of the solid phases in the Co-V system at 298.15 K compared with DFT results at 0 K.

Figure 5 shows the calculated enthalpy of formation at 298.15 K compared to results from the present DFT calculations and DFT databases. This is no surprise since the CALPHAD description is based on the DFT data. Although the DFT data are for 0 K the comparison with the enthalpy calculated for 298 K is valid since no excess heat capacities are used in the description of the phases. Figure 4 shows that the composition of the intermetallic phase is very close to ideal and the homogeneity

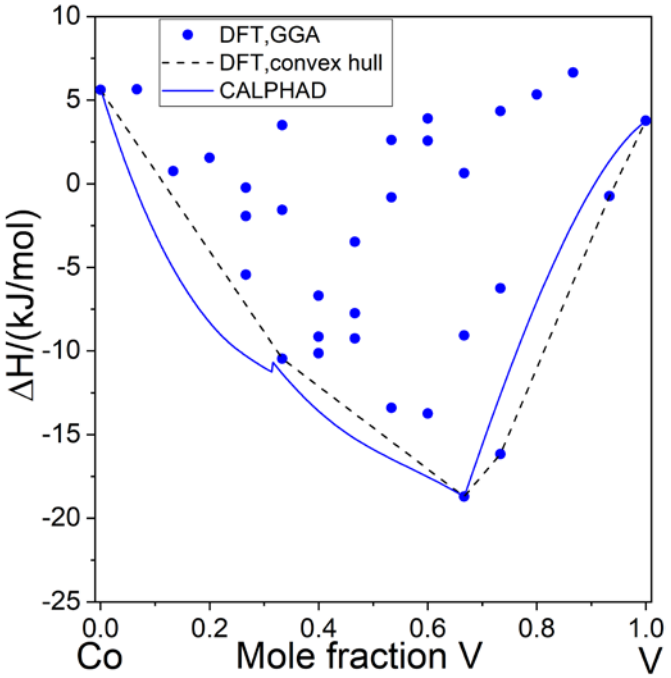

Fig. 6 Calculated enthalpy of formation for the σ phase at 298.15 K compared with the DFT results for all end-members at 0 K.

ranges very narrow indicating that at 298 K substitution on the different sublattices should be small. The comparison of the DFT results from the present DFT calculation and CALPHAD description is shown in Fig. 6. The convex hull from the DFT calculations is well reproduced by the CALPHAD description.

For the description of the metastable ordering of the FCC phase, the DFT values and experimental data from Nagel [14] were adopted. The metastable FCC-$L1_2$ phase diagram is shown in Fig. 7. The calculated congruent FCC-$L1_2$ transition temperature is 1283 K, which is consistent with the experimental data.

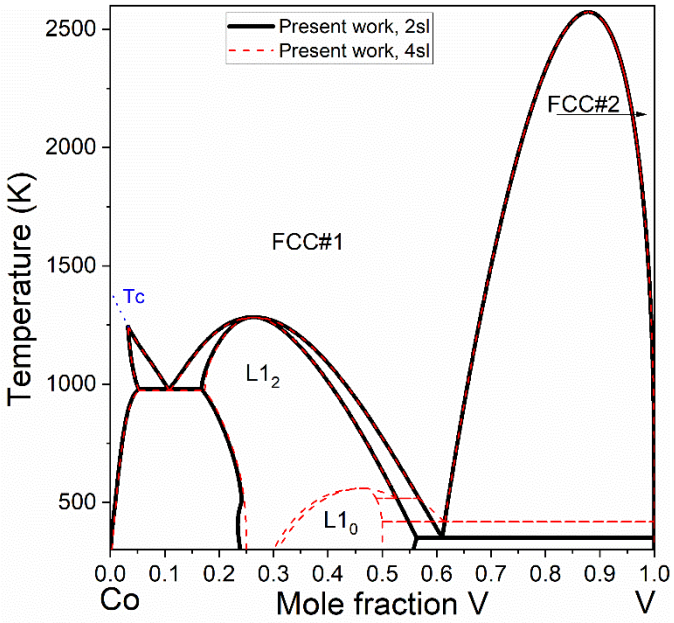

Fig. 7 Calculated metastable FCC-L12 phase diagram

Conclusions

DFT calculations using GGA and spin-polarization were performed to obtain the energies for all end-members of close packed phases in the Co-V system. The energies for the Co_3V, σ and CoV_3 phases were used to assess the parameters for the CALPHAD description. The method to describe the magnetic contribution to the total energy, which has been introduced in our previous work, is described step by step in the present work. G^{σ}_{mag} is included in the description of the end-member compound $\Delta G^{\sigma}_{Co:Co:Co}$, which provides a non-linear description of the magnetic contribution as a function of composition. It needs to be pointed out is that the G^{σ}_{mag} is configuration

dependent. The phase diagram calculated with the present CALPHAD description agrees well with the experimental data.

Acknowledgement

This work was performed under the following financial assistance award 70NANB14H012 from U.S. Department of Commerce, National Institute of Standards and Technology as part of the Center for Hierarchical Materials Design (CHiMaD). TH acknowledges funding from the Deutsche Forschungsgemeinschaft (DFG) through project C1 of the collaborative research centre SFB/TR 103.

References

[1] K. Hilpert, D. Kobertz, V. Venugopal, M. Miller, H. Gerads, F. Bremer, H. Nickel, Phase diagram studies on the Al-Ni system, Z Naturforsch, 42 (1987) 1327-1332.

[2] A. McAlister, The Al-Co (Aluminum-Cobalt) System, J Phase Equiliba, 10 (1989) 646-650.

[3] J. Sato, T. Omori, K. Oikawa, I. Ohnuma, R. Kainuma, K. Ishida, Cobalt-base high-temperature alloys, Science, 312 (2006) 90-91.

[4] S. Kobayashi, Y. Tsukamoto, T. Takasugi, H. Chinen, T. Omori, K. Ishida, S. Zaefferer, Determination of phase equilibria in the Co-rich Co–Al–W ternary system with a diffusion-couple technique, Intermetallics, 17 (2009) 1085-1089.

[5] E.A. Lass, M.E. Williams, C.E. Campbell, K.-W. Moon, U.R. Kattner, γ′ Phase Stability and Phase Equilibrium in Ternary Co-Al-W at 900 °C, J Phase Equilib Diff, 35 (2014) 711-723.

[6] E.A. Lass, R.D. Grist, M.E. Williams, Phase Equilibria and Microstructural Evolution in Ternary Co-Al-W Between 750 and 1100 °C, J Phase Equilib Diff, 4 (2016) 387-401.

[7] K. Ishida, Intermetallic compounds in Co-base alloys–phase stability and application to superalloys, MRS Proc, Cambridge Univ Press, 2009, pp. 1128-U1106-1106.

[8] P. Wang, W. Xiong, U.R. Kattner, C.E. Campbell, E.A. Lass, O.Y. Kontsevoi, G.B. Olson, Thermodynamic re-assessment of the Al-Co-W system, CALPHAD, 59 (2017) 112-130.

[9] C. Nyshadham, C. Oses, J.E. Hansen, I. Takeuchi, S. Curtarolo, G.L.W. Hart, A computational high-throughput search for new ternary superalloys, Acta Mater, 122 (2017) 438-447.

[10] J.J. Ruan, C.P. Wang, S.Y. Yang, T. Omori, T. Yang, Y. Kimura, X.J. Liu, R. Kainuma, K. Ishida, Experimental investigations of microstructures and phase

equilibria in the Co–V–Ta ternary system, J Alloy Compd, 664 (2016) 141-148.

[11] F.L. Reyes Tirado, J. Perrin Toinin, D.C. Dunand, γ+γ′ microstructures in the Co-Ta-V and Co-Nb-V ternary systems, Acta Mater, 151 (2018) 137-148.

[12] G. Liao, F. Yin, Y. Liu, M. Zhao, 1073 K (800 °C) Isothermal Section of the Co-Al-V System, Metall Mater Trans A, 48 (2017) 3904-3911.

[13] Y. Chen, C. Wang, J. Ruan, T. Omori, R. Kainuma, K. Ishida, X. Liu, High-strength Co–Al–V-base superalloys strengthened by γ′-Co3(Al,V) with high solvus temperature, Acta Mater, 170 (2019) 62-74.

[14] L.J. Nagel, B. Fultz, J.L. Robertson, Phase equilibria of Co3 V, J Phase Equilib, 18 (1997) 21.

[15] Automatic Flow for Materials Discovery: AFLOW, http://aflowlib.org/, visited 21-June-2018.

[16] OQMD: The Open Quantum Materials Database, http://oqmd.org/, visited 21-June-2018.

[17] C.E. Campbell, U.R. Kattner, Z.-K. Liu, The development of phase-based property data using the CALPHAD method and infrastructure needs, Integrat Mater Manufact Innov 3(2014) 12.

[18] J. Bratberg, B. Sundman, A thermodynamic assessment of the Co-V system, J Phase Equilib, 24 (2003) 495-503.

[19] S. Huang, L. Li, O.V.d. Biest, J. Vleugels, Thermodynamic assessment of the Co–V and Co–V–C system, J Alloy Compd, 385 (2004) 114-118.

[20] C. Wang, C. Zhao, Y. Lu, T. Li, D. Peng, J. Shi, X. Liu, Experimental observation of magnetically induced phase separation and thermodynamic assessment in the Co–V binary system, Mater Chem Phys, 162 (2015) 555-560.

[21] J.F. Smith, The Co-V (Cobalt-Vanadium) System, J Phase Equilib, 12 (1991) 324-331.

[22] P. Wang, M.C. Peters, U.R. Kattner, K. Choudhary, G.B. Olson, Thermodynamic analysis of the topologically close packed σ phase in the Co-Cr system, Intermetallics, 105 (2019) 13-20.

[23] T. Hammerschmidt, A.F. Bialon, D.G. Pettifor, R. Drautz, Topologically close-packed phases in binary transition-metal compounds: matching high-throughput ab initio calculations to an empirical structure map, New J Phys, 15 (2013) 115016.

[24] G. Kresse, J. Hafner, Ab initio molecular-dynamics simulation of the liquid-metal-amorphous-semiconductor transition in germanium, Phys Rev B, 49 (1994) 14251-14269.

[25] G. Kresse, J. Furthmüller, Efficient iterative schemes for ab initio total-energy calculations using a plane-wave basis set, Phys Rev B, 54 (1996) 11169-11186.

[26] P.E. Blöchl, O. Jepsen, O.K. Andersen, Improved tetrahedron method for Brillouin-zone integrations, Phys Rev B, 49 (1994) 16223.

[27] J.P. Perdew, K. Burke, M. Ernzerhof, Generalized gradient approximation made simple, Phys Rev Lett, 77 (1996) 3865-3868.

[28] Scientific Group Thermodata Europe: SGTE, https://www.sgte.net/en/free-pure-substance-database, visited 21-June-2018.

[29] A.T. Dinsdale, SGTE data for pure elements, CALPHAD, 15 (1991) 317-425.

[30] O. Redlich, A.T. Kister, Algebraic representation of thermodynamic properties and the classification of solutions, Ind Eng Chem, 40 (1948) 345-348.

[31] M. Hillert, M. Jarl, A model for alloying in ferromagnetic metals, CALPHAD, 2 (1978) 227-238.

[32] I. Ansara, B. Burton, Q. Chen, M. Hillert, A. Fernandez-Guillermet, S.G. Fries, H.L. Lukas, H.-J. Seifert, W.A. Oates, Models for composition dependence, CALPHAD, 24 (2000) 19-40.

[33] M. Hillert, The compound energy formalism, J Alloy Compd, 320 (2001) 161-176.

[34] A. Kusoffsky, N. Dupin, B. Sundman, On the compound energy formalism applied to fcc ordering, CALPHAD, 25 (2001) 549-565.

[35] P.A. Korzhavyi, B. Sundman, M. Selleby, B. Johansson, Atomic, electronic, and magnetic structure of iron-based sigma-phases, MRS Proceedings, Cambridge Univ Press, 2004, pp. S4. 10.

[36] R. Lizárraga, F. Pan, L. Bergqvist, E. Holmström, Z. Gercsi, L. Vitos, First principles theory of the hcp-fcc phase transition in cobalt, Sci Rep, 7 (2017) 3778.

[37] A.I. Liechtenstein, M. Katsnelson, V. Antropov, V. Gubanov, Local spin density functional approach to the theory of exchange interactions in ferromagnetic metals and alloys, J Magn Magn Mater, 67 (1987) 65-74.

[38] Thermo-Calc Software, http://www.thermo-calc.com, visited 21-June-2018.

[39] M.V. Nevitt, P.A. Beck, Curie Temperatures of Binary and Ternary Sigma Phases, JOM, 7 (1955) 669-674.

[40] P. Villars, Pearson's handbook: Desk edition: Crystallographic data for intermetallic phases, ASM international Materials Park, OH1997.

Tables

Table 1 Summary of the crystallographic information for the phases of the Co-V system [40]

Phase name	Crystallographic information			
	Strukturbericht.	Prototype	Pearson symbol	Space group
FCC, γ or αCo	A1	Cu	cF4	Fm-3m
HCP, εCo	A3	Mg	hP2	P63/mmc
(V)	A2	W	cI2	Im-3m
Co_3V		$PuAl_3$	hP24	P63/mmc
σ	$D8_b$	σCrFe	tP30	$P4_2/mnm$
CoV_3	A15	Cr_3Si	cP8	Pm-3n
$L1_2$	$L1_2$	Cu_3Au	cP4	Pm-3m

Table 2 Enthalpies of formation, $\Delta G^{\phi}_{i:j:k:l:m}$ in J/mol (mole of atoms) of all end-members of the Co3V, σ, CoV3 phases obtained from the DFT calculations $\Delta G^{\phi}_{i:j:k:l:m}$.

Phase	Wyckoff Positions					
Co_3V	Co	Co	Co	Co		1102.6
	V	V	V	V		23284.4
	V	Co	Co	Co		-0.6
	Co	Co	Co	V	-	-1360.4
	Co	V	Co	V	-	4514.9
	Co	V	Co	Co	-	1791.4
	Co	Co	V	Co	-	-7137.4
	Co	Co	V	V	-	-16310
	V	V	Co	Co	-	7001.7
	Co	V	V	Co	-	-7005.5
	Co	V	V	V	-	-7297.6
	V	Co	Co	V	-	4421.7
	V	V	Co	V	-	13938.7
	V	Co	V	V	-	9887.2
	V	V	V	Co	-	17389.9
	V	Co	V	Co	-	8496.7
CoV_3	Co	Co	-	-	-	9184.9
	V	Co	-	-	-	-2651.9
	Co	V	-	-	-	-18960
	V	V	-	-	-	4642
σ	V	Co	Co	Co	Co	5621.7
	Co	V	Co	Co	Co	756.2
	V	V	Co	Co	Co	1547.3
	Co	Co	Co	Co	V	-1919.2
	Co	Co	Co	V	Co	-228.9
	Co	Co	V	Co	Co	-5412.2

	V	Co	Co	Co	V	-1553.3
	V	Co	Co	V	Co	3490.7
	V	Co	V	Co	Co	-10421
	Co	V	Co	Co	V	-10088
	Co	V	Co	V	Co	-9112.4
	Co	V	V	Co	Co	-6661.9
	V	V	Co	Co	V	-7702.4
	V	V	Co	V	Co	-3455.5
	V	V	V	Co	Co	-9210.2
	Co	Co	Co	V	V	-809.3
	Co	Co	V	Co	V	-13348
	Co	Co	V	V	Co	2609.4
	V	Co	Co	V	V	2566.1
	V	Co	V	Co	V	-13689
	V	Co	V	V	Co	3892.4
	Co	V	Co	V	V	-9040.3
	Co	V	V	Co	V	-18631
	Co	V	V	V	Co	632.3
	V	V	Co	V	V	-6224.5
	V	V	V	Co	V	-16089
	V	V	V	V	Co	4325.1
	Co	Co	V	V	V	5316.9
	V	Co	V	V	V	6622.4
	Co	V	V	V	V	-734.9
	Co	Co	Co	Co	Co	5591.7
	V	V	V	V	V	3753.3
FCC	Co	Co	Co	Co		1706.8
	V	Co	Co	Co		-15766
	V	V	Co	Co		-13103
	V	V	V	Co		7017.6
	V	V	V	V		23393.3

Table 3 Phase names, models (sublattice formulae) and parameters of the present thermodynamic description. Gibbs energy is given in J/mol (mole of formula units according to the sublattice definition), temperature (T) in K

Liquid: $(Co,V)_1$
$L_{Co,V}^{0,Liquid}$= -60297.6+2.6502$\cdot T$; $L_{Co,V}^{1,Liquid}$ =-10417.3; $L_{Co,V}^{2,Liquid}$=+18698.7
(Ta) (BCC_A2): $(Co,V,Va)_1(Va)_3$
$L_{Va:Va}^{0,BCC_{A2}}$ =30$\cdot$T; $L_{Co,Va:Va}^{0,BCC_{A2}}$ =46912; $L_{V,Va:Va}^{0,BCC_{A2}}$ =80000; $L_{Co,V:Va}^{0,BCC_{A2}}$ = -62617.3+12.1461$\cdot T$; $L_{Co,Ta:Va}^{1,BCC_{A2}}$ =-18518.3
(αCo)(γ) (FCC_A1): $(Co,V)_1(Va)_1$
$L_{Co,V}^{0,FCC_{A1}}$= -69595.2+11.2314 $\cdot T$; $L_{Co,V}^{1,FCC_{A1}}$= -41802.8+4.2329 $\cdot T$; $L_{Co,V}^{2,FCC_{A1}}$=29000 $TC_{Co,Ta}^{0,FCC_{A1}}$=-2500; $TC_{Co,Ta}^{1,FCC_{A1}}$=-1000
Co_3V: $(Co,V)_{0.75}(Co,V)_{0.25}$
$\Delta G_{Co:Co}^{Co_3V}$ = 1102+1$\cdot$ $G_{Co}^{\circ,HSER}(T)$; $\Delta G_{Co:V}^{Co_3V}$ = -22766.5+5.0540$\cdot T$ +0.75$\cdot G_{Co}^{\circ,HSER}(T)$+0.25$\cdot G_{V}^{\circ,HSER}(T)$; $\Delta G_{V:V}^{Co_3V}$ = 23284+1$\cdot G_{V}^{\circ,HSER}(T)$; $\Delta G_{V:Co}^{Co_3V}$ = 4752 +0.25$\cdot G_{Co}^{\circ,HSER}(T)$+0.75$\cdot G_{V}^{\circ,HSER}(T)$; $L_{Co,V:V}^{Co_3V}$=-33511.3; $L_{Co:Co,V}^{Co_3V}$=20000
σ: (**Co**,V)$_{0.533333}$ (Co,**V**)$_{0.333334}$ (Co,**V**)$_{0.133333}$ $^{o}G_{Co}^{dis\_\sigma}$=6958+$G_{\mathrm{Co}}^{\circ,\mathrm{HSER}}(T)$; $^{o}G_{V}^{dis\_\sigma}$=3768.4+$G_{\mathrm{V}}^{\circ,\mathrm{HSER}}(T)$; $G_{Co,V}^{0,dis\_\sigma}$=-27066.3; $G_{Co,V}^{1,dis\_\sigma}$=-65628.6 $\Delta G_{Co:Co:Co}^{\sigma}$=0; $TC_{Co:Co:Co}^{\sigma}$=1400; $\beta_{Co:Co:Co}^{\sigma}$=1.66

$\Delta G^{\sigma}_{\mathrm{V:Co:Co}}$ =-16992.9+4.8088·T; $\Delta G^{\sigma}_{\mathrm{Co:V:Co}}$ =2798.0; $\Delta G^{\sigma}_{\mathrm{V:V:Co}}$ =-1115.8; $\Delta G^{\sigma}_{\mathrm{Co:Co:V}}$=-4478.8+5.1637·$T$; $\Delta G^{\sigma}_{\mathrm{V:Co:V}}$= -25228.3+2.8157 ·$T$; $\Delta G^{\sigma}_{\mathrm{Co:V:V}}$= -5663.7

CoV_3: $(Co)_{0.25}(V)_{0.75}$

$\Delta G_f^{CoV_3}$= -28118.3+7.5228·T+0.25·$G_{Co}^{\circ,HSER}(T)$+0.75·$G_V^{\circ,HSER}(T)$

$L1_2$ $(Co,V)_{0.25}(Co,V)_{0.25}(Co,V)_{0.25}(Co,V)_{0.25}$

CEF order/disorder formalism[34]

u_{AB} = -4498.5+0.7535·T; $\Delta G^{L1_2}_{Co_3V}$=3 u_{AB}; $\Delta G^{L1_2}_{Co_2V_2}$=4 u_{AB}+9034.8;

$\Delta G^{L1_2}_{CoV_3}$= 3 u_{AB} +20495.5-2.2605·T = 7000

Table 4: Configuration of the σ phase and ΔG_{mag} at x(V)=0.134 and T = 298.15 K

	Site occupation of σ phase			ΔG_{mag} (J/mol)
	Site 1	Site 2	Site 3	
Pre-CALPHAD	0.999	1.0	1.0	0
Full-assessment	0.748	1.0	1.0s	-3849